Mechanical Systems and Signal Processing 216 (2024) 111428

Contents lists available at ScienceDirect

Mechanical Systems and Signal Processing

journal homepage: www.elsevier.com/locate/ymssp

A novel mirror-assisted method for full-field vibration measurement of a hollow cylinder using a three-dimensional continuously scanning laser Doppler vibrometer system

K. Yuan, W.D. Zhu *

Department of Mechanical Engineering, University of Maryland, Baltimore County, 1000 Hilltop Circle, Baltimore, MD 21250, United States

ARTICLE INFO

Keywords:
3D CSLDV system
Mirror-assisted testing method
Hollow cylinder
Vibration stitching
Full-field measurement
Panoramic 3D operating deflection shape

ABSTRACT

A novel general-purpose three-dimensional (3D) continuously scanning laser Doppler vibrometer (CSLDV) system was recently developed by the authors to measure 3D vibration of a structure with a curved surface. As a non-contact system, it can avoid the mass-loading problem in 3D vibration measurement using triaxial accelerometers. In previous studies, the 3D CSLDV system was used to measure 3D full-field vibration of a turbine blade with a curved surface and identify its operating deflection shapes (ODSs) and mode shapes. The 3D CSLDV system had the same level of accuracy as that with a commercial 3D scanning laser Doppler vibrometer system, but can measure many more points in much less time than the latter. However, the 3D CSLDV system can be limited by its field of view, which is a common problem for optical-based measurement devices. Moving the 3D CSLDV system to different positions to measure different parts of a test structure is not practical during 3D CSLDV measurement, since the system has to be re-calibrated once it has been moved, which can be time-consuming and introduce measurement errors. This work proposes a novel mirror-assisted testing methodology for 3D CSLDV measurement that aims to measure vibration of difficult-to-access areas of a structure without moving the 3D CSLDV system during the test, and stitch ODSs of its different parts together to obtain its panoramic 3D ODSs. The proposed methodology includes a novel scan trajectory design method that uses virtual areas of the structure behind the mirror to conduct continuous and synchronous scanning of three laser spots, and a novel velocity transformation method that uses virtual positions of three laser heads behind the mirror to stitch ODSs of different parts of the structure together. To demonstrate the proposed methodology, 3D CSLDV measurement is conducted on an aluminum hollow cylinder specimen, which has difficult-to-access areas such as its side and back surfaces, with the assistance of the mirror to obtain its panoramic 3D ODSs corresponding to its first two modes. Comparison between identified ODSs of the hollow cylinder specimen from the experiment and mode shapes from its finite element model is made and modal assurance criterion values are larger than 0.98.

1. Introduction

A continuously scanning laser Doppler vibrometer (CSLDV) was developed to significantly improve efficiency and spatial

* Corresponding author.
E-mail addresses: kyuan1@umbc.edu (K. Yuan), wzhu@umbc.edu (W.D. Zhu).

https://doi.org/10.1016/j.ymssp.2024.111428
Received 3 August 2023; Received in revised form 28 February 2024; Accepted 11 April 2024
Available online 2 May 2024

resolution of vibration measurement of a structure [1]. The CSLDV was made by adding two orthogonal scan mirrors in front of a single-point laser Doppler vibrometer. Two scan mirrors can be referred to as X and Y mirrors based on their rotation axes, respectively. During CSLDV measurement, two scan mirrors can be controlled to continuously rotate about their rotation axes, and the laser spot of the CSLDV can continuously move along a pre-designed scan trajectory on the structure, which is a major difference compared to a conventional scanning laser Doppler vibrometer (SLDV) system that has a point-by-point scanning capability. Researchers who focused on this area developed various methods for processing response of a structure from CSLDV measurement and identifying its operating deflection shapes (ODSs) and modal parameters [2–6]. Dense vibration of a structure from CSLDV measurement can be used to identify its damages via curvatures of its ODSs [7] or mode shapes [8].

Above studies mainly focused on using a CSLDV with one laser head, which can be referred to as a 1D CSLDV, to measure transverse vibration of a structure. One approach to measure 3D vibration of the structure is to place the laser head of the CSLDV at three independent positions and transform measured velocity response to three components along three orthogonal directions of a coordinate system [9,10]. Weekes and Ewins [9] measured 3D vibration of a turbine blade under multi-sine excitation using the CSLDV with the assistance of a Microsoft Kinect. Chen and Zhu [10] proposed a novel calibration method and a velocity transformation method to measure 3D vibration of a beam, and reported good agreement between 3D vibration components from CSLDV measurement and those from a commercial Polytec 3D SLDV PSV-500-3D. Recently, a novel 3D CSLDV system with three laser heads was developed by the authors' group to measure 3D vibration of a structure [11,12,6]. Experimental investigations were conducted on beams and plates by using the 3D CSLDV system to identify their ODSs and modal parameters such as natural frequencies and mode shapes. Experimental results showed that the 3D CSLDV system had the same level of accuracy as that of a commercial Polytec 3D SLDV PSV-500-3D system, but had much higher measurement efficiency than the latter. The 3D CSLDV system was subsequently improved to measure 3D ODSs [13] and mode shapes [14] of a turbine blade with a curved surface. A novel scan trajectory design method based on the 3D profile of the structure and calibration results of the 3D CSLDV system was developed in these studies, and 3D CSLDV measurements were conducted on the turbine blade to identify its ODSs under sinusoidal excitation and its mode shapes under random excitation. However, the 3D CSLDV system can be limited by its field of view (FOV), which is a common problem for optical-based measurement devices, and cannot obtain full-field vibration of a structure with difficult-to-access areas, such as side and back surfaces of a cylindrical structure. Moving the 3D CSLDV system to different positions to measure different parts of the structure is not practical during 3D CSLDV measurement, since the system needs be re-calibrated once it is moved, which is time-consuming and can introduce measurement errors.

Chen et al. [15] developed an experimental modal testing approach to obtain and stitch mode shapes of both surfaces of a turbine blade together using a SLDV system with the assistance of four alignment objects. The SLDV system was moved once in the experiment to measure vibration of the back side of the turbine blade. However, the proposed method is a two-surface measurement technique and can only be applied to a structure with two parallel surfaces. Another approach to extend the FOV of an optical-based measurement device, such as a digital image correlation (DIC) system and a laser Doppler vibrometer, is using a mirror or multiple mirrors. The major advantage of a mirror-assisted method is that it can be used to measure deformation or vibration of multiple surfaces of a structure and obtain its panoramic deformation or vibration shapes without moving the measurement system. During DIC measurement, deformation of a difficult-to-access area of the structure can be captured via its virtual image behind the mirror. Pan and Chen [16,17] developed a multi-view DIC method with the assistance of two orthogonal planar mirrors. Methods for transformation and reconstruction of virtual surfaces of the structure to and at their real positions, respectively, were proposed in their studies. The methodology was used in material tests of a planar and a cylindrical specimen, respectively, to provide their panoramic shapes and deformations. However, the above studies on DIC measurement focused on static tests of structures. Moreover, mandatory spaces between the specimen and the mirrors can ensure that the back surface of the specimen is visible, but can lead to depth differences among real and virtual images. A laser vibrometer is not limited by the depth problem since it has a wider range of the measurement distance than a camera for DIC measurement.

To measure vibration of a structure with difficult-to-access areas, a SLDV system can be used with the assistance of a mirror or multiple mirrors. Witt et al. [18] conducted full-field strain measurement of a joined aluminum assembly that contained two C-channel legs and a flat top member using a 3D SLDV system and two mirrors, where two measured surfaces were orthogonal to each other. Yuan and Zhu [19] measured dual-surface vibration of a pyramidal truss sandwich panel using a 3D SLDV system and a mirror to identify its mode shapes and validate its finite element (FE) model. However, both structures in the above studies had flat surfaces and the SLDV system had a point-by-point scanning mode. In SLDV measurement using mirrors for full-field measurement, the commercial software by Polytec provides a feature in 3D alignment by checking the "mirror" option and another feature in post-processing to stitch ODSs of different parts of the test structure together by using the "combine" option. However, while the user can obtain stitched full-field ODSs of the structure shown on its reconstructed surface, the theories behind these features are not available in the literature and unknown to the user. Moreover, signal processing algorithms for CSLDV measurement are not available in the Polytec software. For 3D full-field CSLDV measurement using mirrors, more customized parameters of the test structure, which are not available in the Polytec software, are needed to improve 3D CSLDV measurement without using mirrors [6,11–14]. For instance, the previous scan trajectory design method is improved in this work to incorporate mirrors by using virtual coordinates of the structure behind mirrors, and the previous velocity transformation method is improved in this work by using coordinates of incident points of laser beams on mirrors. Therefore, both the commercial Polytec software and the 3D CSLDV method without using mirrors cannot be directly used for the case in this work. It is another challenge to conduct 3D vibration measurement of a structure with curved and difficult-to-access areas, such as a cylindrical structure, using the 3D CSLDV system. Using a 360°-oscillating stand to support the cylindrical structure [20] and placing a continuously-rotating 45° mirror inside the cylindrical structure [20–22] are two methodologies developed to measure full-field vibration of the structure using the 1D CSLDV. However, the former is not practical for a large and heavy-weight structure since it cannot

be easily moved by the oscillating stand, and the limitation of the latter is that the cylindrical structure must be hollow and have a relatively large inner space for placing the rotating mirror inside it.

This work aims to extend the FOV of the recently developed general-purpose 3D CSLDV system by the authors [13,14]. A novel mirror-assisted testing methodology for 3D CSLDV measurement is proposed in this work to measure vibration of difficult-to-access areas of a structure without moving the 3D CSLDV system during the test and stitch ODSs of its different parts together to obtain its panoramic 3D ODSs. There are two novelties in this work. The first novelty is improving the scan trajectory design method to fit measurement on difficult-to-access areas of the structure based on coordinates of their virtual images in the mirror. The second novelty is improving the velocity transformation method by using virtual positions of three laser heads. The major advancement of the proposed method over previous studies is avoiding moving both the test structure and the 3D CSLDV system, which can introduce measurement errors. Moreover, a large inner space of the test structure is not required. The proposed method can therefore be used in more general scenarios in practice.

The remainder of this paper is structured as follows. The novel mirror-assisted 3D CSLDV system for measuring vibration of difficult-to-access areas of a structure is introduced in Section 2, where methodologies for measuring vibration of areas in and out of the FOV of the 3D CSLDV system are shown in Sections 2.1 and 2.2, respectively, and the methodology for velocity transformation of different areas of the structure is shown in Section 2.3. Experimental validation of the mirror-assisted methodology for the 3D CSLDV system is conducted on a cylindrical structure and shown in Section 3. Conclusions are drawn in Section 4.

2. Methodology for using the mirror-assisted 3D CSLDV system

The testing principle of the proposed mirror-assisted 3D CSLDV system is shown in Fig. 1. It is extended from the general-purpose 3D CSLDV system recently developed by the authors' group [13,14], which contains three laser heads and an external controller, and can be used to measure 3D vibration of a structure with a curved surface. The laser head I shown in Fig. 1 has an internal range finder that can measure the 3D profile of the test structure with a curved surface. Scan mirror signals can be calculated using the spatial relation among three laser heads and the 3D profile of the structure, and inputted into the external controller to direct three laser spots to synchronously and continuously move along a desired scan trajectory on the surface of the structure. Velocities of a measurement point on the structure obtained by three laser heads can be transformed to a pre-defined global measurement coordinate system (MCS). Therefore, 3D vibration of the curved surface of the test structure that is in the FOV of the 3D CSLDV system, as shown in Fig. 1, can be directly measured. To direct laser spots of three laser heads to scan an area that is out of the FOV of the 3D CSLDV system, a mirror can be used to reflect their laser beams by adjusting its position and orientation, as shown in Fig. 1. The methodology developed in previous studies [11,13] for calibrating the 3D CSLDV system is briefly introduced in the Appendix. Outputs of the system calibration are three pairs of the **R** matrix and the **T** vector, which are the direction cosine matrix and the translation vector, respectively, to connect the MCS with the vibrometer coordinate system (VCS). Note that these outputs of the calibration are significant parameters for measurement using the 3D CSLDV system, and cannot be obtained from the standard calibration in the Polytec commercial software, which includes 1) a 2D alignment that aims to recognize the test area through its 2D image and align three laser spots together, and 2) a 3D alignment that aims to determine coordinates of points on the test area. While the 3D CSLDV calibration has the same goal as that in the Polytec commercial software, they have different methodologies with the former focusing on geometrical relations and the latter focusing on image processing.

2.1. Vibration measurement of an area in the FOV of the system

As shown in Fig. 2, the entire surface of the test structure, which is a hollow cylinder specimen in this work, can be divided into four areas. The area A1 is in the FOV of the 3D CSLDV system and areas A2-A4 are out of its FOV. This section shows the methodology for measuring vibration of the area A1 of the structure using the 3D CSLDV system. To conduct a synchronous scanning on the curved surface of the structure, coordinates of three laser spots of three laser heads are assumed to be the same in the MCS when they move

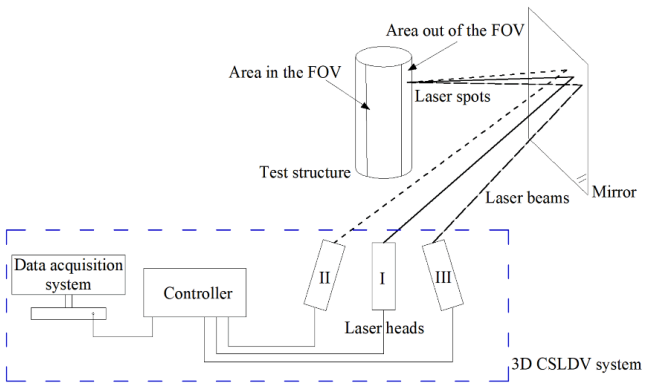

Fig. 1. Testing principle of the mirror-assisted 3D CSLDV system.

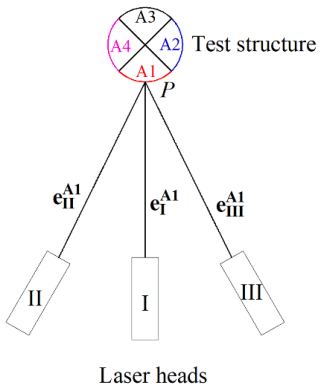

Fig. 2. Schematic of vibration measurement of the area A1 of the test structure, which is in the FOV of the 3D CSLDV system.

along the scan trajectory. Therefore, Eq. (A1) can be further written as

$$\mathbf{P}_{\mathrm{MCS}} = \mathbf{R}_{\mathrm{I}}\mathbf{P}_{\mathrm{VCS\_I}} + \mathbf{T}_{\mathrm{I}} = \mathbf{R}_{\mathrm{II}}\mathbf{P}_{\mathrm{VCS\_II}} + \mathbf{T}_{\mathrm{II}} = \mathbf{R}_{\mathrm{III}}\mathbf{P}_{\mathrm{VCS\_III}} + \mathbf{T}_{\mathrm{III}} \tag{1}$$

where subscripts I, II, and III are indices of three laser heads. In this work, the 3D profile of the area A1 of the test structure can be obtained using the laser head I with its internal ranger finder. When the laser spot of the laser head I is directed to a profile point, corresponding rotation angles of scan mirrors α and β, and the distance r can be recorded. Eqs. (A1) and (A2) can then be used to obtain coordinates of all profile points of the area A1in the MCS, which construct its 3D profile. To conduct a continuous scan along the scan trajectory, coordinates of measurement points in the MCS can be obtained by interpolating the 3D profile of the test structure. Coordinates of each measurement point in VCSs of three laser heads $\mathbf{P}_{\mathrm{VCS\_I}}$, $\mathrm{P}_{\mathrm{VCS\_II}}$, and $\mathrm{P}_{\mathrm{VCS\_III}}$ can be obtained by substituting their **R** and **T** matrices from the system calibration into Eq. (A1). Rotation angles of scan mirrors in three laser heads can then be obtained by

$$\alpha_{\mathrm{I}} = \arctan\left(z_{\mathrm{VCS\_I}}/y_{\mathrm{VCS\_I}}\right), \beta_{\mathrm{I}} = \arctan\left(x_{\mathrm{VCS\_I}}/\left(y_{\mathrm{VCS\_I}}/\cos\alpha_{\mathrm{I}}\text{-}d\right)\right) \tag{2a}$$

$$\alpha_{\mathrm{II}} = \arctan\left(z_{\mathrm{VCS\_II}}/y_{\mathrm{VCS\_II}}\right), \beta_{\mathrm{II}} = \arctan\left(x_{\mathrm{VCS\_II}}/\left(y_{\mathrm{VCS\_II}}/\cos\alpha_{\mathrm{II}}\text{-}d\right)\right) \tag{2b}$$

$$\alpha_{\mathrm{III}} = \arctan\left(z_{\mathrm{VCS\_III}}/y_{\mathrm{VCS\_III}}\right), \beta_{\mathrm{III}} = \arctan\left(x_{\mathrm{VCS\_III}}/\left(y_{\mathrm{VCS\_III}}/\cos\alpha_{\mathrm{III}}\text{-}d\right)\right) \tag{2c}$$

Finally, continuous and synchronous scanning can be conducted on the area A1 by feeding rotation angles back to three laser heads, and three time-velocity series $V_{\mathrm{I}}^{\mathrm{A1}}$, $V_{\mathrm{II}}^{\mathrm{A1}}$, and $V_{\mathrm{III}}^{\mathrm{A1}}$, where the superscript A1 denotes the corresponding area number, can be acquired by three laser heads, which completes vibration measurement on the area A1. While the above theory was developed in authors' previous work, it is improved in Section 2.2 to incorporate mirrors in 3D CSLDV measurement.

2.2. *Vibration measurement of an area out of the FOV of the 3D CSLDV system*

This section illustrates the methodology for measuring vibration of areas A2-A4 of the test structure using the 3D CSLDV system, as shown in Fig. 3. For each area, the mirror is placed at an appropriate position and its orientation is manually adjusted to ensure that all three laser spots can reach the entire area, and the mirror is fixed during measurement of the area. In this section, coordinates of virtual

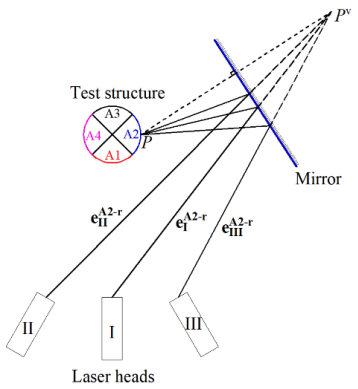

Fig. 3. Schematic of vibration measurement of the area A2 of the test structure, which is out of the FOV of the 3D CSLDV system.

points P^{v} of areas A2-A4 behind the mirror can be obtained in the MCS by the laser head I using the method based on rotation angles of scan mirrors and distances mentioned in the previous section. Coordinates of corresponding points on real areas A2-A4 can be obtained by mirroring those of virtual points about the mirror plane and used to reconstruct the panoramic surface of the test structure and recover vibration of virtual surfaces to the actual coordinate system. Based on the reflective configuration of the mirror, coordinates of virtual points $\mathbf{P}^{v}_{MCS}$ are used to replace their corresponding real points in Eq. (1) to conduct continuous and synchronous scanning on areas A2-A4, which yields

$$\mathbf{P}^{v}_{MCS} = \mathbf{R}_{I}\mathbf{P}^{v}_{VCS\_I} + \mathbf{T}_{I} = \mathbf{R}_{II}\mathbf{P}^{v}_{VCS\_II} + \mathbf{T}_{II} = \mathbf{R}_{III}\mathbf{P}^{v}_{VCS\_III} + \mathbf{T}_{III} \tag{3}$$

Similarly, rotation angles of scan mirrors in laser heads can be determined using corresponding $\mathbf{P}^{v}_{VCS}$ and Eqs. 2(a)-2(c), and fed back to laser heads to conduct continuous and synchronous scanning on areas A2-A4. Time-velocity series acquired for areas A2-A4 can be denoted as $V_{I}^{A2/A3/A4}$, $V_{II}^{A2/A3/A4}$, and $V_{III}^{A2/A3/A4}$.

2.3. Velocity transformation of different areas of the test structure

As shown in Fig. 2, directly acquired time-velocity series V_{I}^{A1}, V_{II}^{A1}, and V_{III}^{A1} of the area A1 are acquired along laser beams of three laser heads, respectively, whose unit directional vectors $\mathbf{e}_{I}^{A1}$, $\mathbf{e}_{II}^{A1}$, and $\mathbf{e}_{III}^{A1}$ can be determined by substituting corresponding rotation angles into Eq. (3). Time-velocity series V_{I}^{A1}, V_{II}^{A1}, and V_{III}^{A1} can then be transformed to velocity components along x, y, and z directions of the global MCS by

$$\left[V_{x}^{A1}, V_{y}^{A1}, V_{z}^{A1}\right]^{T} = \left[\mathbf{R}_{I}\mathbf{e}_{I}^{A1}, \mathbf{R}_{II}\mathbf{e}_{II}^{A1}, \mathbf{R}_{III}\mathbf{e}_{III}^{A1}\right]^{T}\left[V_{I}^{A1}, V_{II}^{A1}, V_{III}^{A1}\right]^{T} \tag{4}$$

where the superscript T denotes transpose of a matrix. Acquired velocities of areas A2-A4 are along directions from measurement points P to virtual positions of laser heads behind the mirror. For instance, as shown in Fig. 4, time-velocity series V_{I}^{A2}, V_{II}^{A2}, and V_{III}^{A2} of a point P on the area A2 are along virtual unit directional vectors $\mathbf{e}_{I}^{A2\text{-}v}$, $\mathbf{e}_{II}^{A2\text{-}v}$, and $\mathbf{e}_{III}^{A2\text{-}v}$, respectively. Taking $\mathbf{e}_{I}^{A2\text{-}v}$ of the laser head I as an example, one has

$$\mathbf{e}_{I}^{A2\text{-}v} = \frac{\mathrm{PM}_{I}^{A2}}{\left|\mathrm{PM}_{I}^{A2}\right|} \tag{5}$$

where M_{I}^{A2} denotes the incident point of the laser beam of the laser head I on the mirror for the area A2. It is actually the intersection point of the line that is from the laser head I to the virtual point P^{v} and the plane of the mirror. Therefore, its coordinates can be determined by using P^{v}, $\mathbf{e}_{I}^{A2\text{-}r}$, and $\mathbf{n}$, where $\mathbf{e}_{I}^{A2\text{-}r}$ can be determined by substituting corresponding rotation angles into Eq. (A3), and $\mathbf{n}$ is the normal vector of the mirror plane that can be determined using any three points on the mirror. By obtaining $\mathbf{e}_{I}^{A2\text{-}v}$, $\mathbf{e}_{II}^{A2\text{-}v}$, and $\mathbf{e}_{III}^{A2\text{-}v}$, time-velocity series V_{I}^{A2}, V_{II}^{A2}, and V_{III}^{A2} can be transformed to velocity components along x, y, and z directions of the global MCS by

$$\left[V_{x}^{A2}, V_{y}^{A2}, V_{z}^{A2}\right]^{T} = \left[\mathbf{e}_{I}^{A2\text{-}v}, \mathbf{e}_{II}^{A2\text{-}v}, \mathbf{e}_{III}^{A2\text{-}v}\right]^{T}\left[V_{I}^{A2}, V_{II}^{A2}, V_{III}^{A2}\right]^{T} \tag{6}$$

By applying above methods based on virtual measurement points and virtual laser heads, measured vibration of areas A2-A4 can be recovered to the global MCS and reconstructed with their real coordinates.

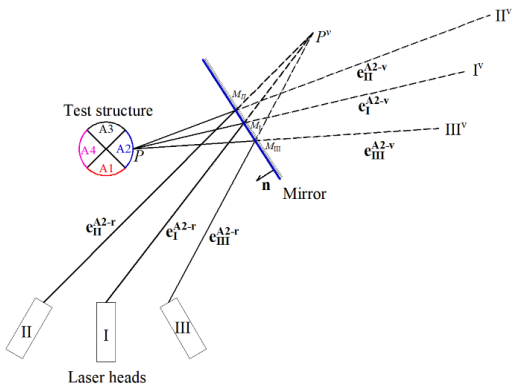

Fig. 4. Schematic of velocity transformation for the area A2 of the test structure, which is out of the FOV of the 3D CSLDV system.

3. Experimental validation

An aluminum hollow cylinder specimen was used as the test structure in this work to validate the proposed mirror-assisted testing method using the 3D CSLDV system. It had a height of 205 mm, an inner diameter of 69.7 mm, and an outer diameter of 76 mm. As shown in Figs. 5(a)–(c), two strings were used to hang the hollow cylinder specimen to simulate its free boundaries, and a speaker was used to excite the specimen using sinusoidal excitation with frequencies that are close to its natural frequencies. A grey reflective tape was attached on the outer surface of the hollow cylinder specimen to maximize back-scattering of laser light. A mirror was mounted to an adjustable frame and placed at a side of the hollow cylinder specimen. The mirror used in this work is a high-quality flat laser mirror provided by Polytec to avoid the distortion issue that can make three laser spots non-synchronous during continuous scanning. As discussed in Section 2, its orientation at each position was manually adjusted to ensure that all three laser spots can reach the entire desired area through its reflection. Therefore, the number of areas for the surface of the test structure, which is four in this experiment, mainly depends on the curvature of its surface. Note that Fig. 5(a) showed the position and orientation of the mirror corresponding to measurement for the area A2, and the mirror was then moved to next positions corresponding areas A3 and A4, as shown in Figs. 5(b) and (c), respectively, to complete full-field measurement. Alignment of laser spots is checked by looking at the back of the test structure, as it is a more straightforward way than looking in the mirror. Laser spots were re-focused before scanning and measuring on each area, as use of the mirror changed stand-off distances between laser heads and measured areas. Considerations in the experimental setup for minimizing vibration of the mirror include using a heavy base to stabilize the adjustable frame and placing the mirror at sides of the speaker to avoid direct excitation from the speaker. Moreover, sinusoidal excitation with frequencies of 1524 Hz and 1593 Hz was used in the experiment, which were the first two natural frequencies of the cylindrical specimen, but not natural frequencies of the mirror. Responses in the frequency domain of the test structure, and those of the mirror at its three positions under periodic chirp excitation with a frequency range of [0, 2000] Hz from the speaker are shown in Fig. 6. One could see that no peak around 1524 Hz and 1593 Hz could be found in frequency spectra of the mirror at its three positions. As these excitation frequencies are high frequencies for the mirror, vibration introduced by them is small for the mirror in the experiment.

The workflow of 3D CSLDV measurement of the hollow cylinder specimen using the proposed mirror-assisted testing method is shown in Fig. 7. The Polytec software was used in steps 1 and 2 when its range finder was needed to determine coordinates of reference points and measurement points, and in step 3 for data acquisition. The external controller MicroLabBox and its software ControlDesk were also used in steps 1 through 3 to input and record rotation angles of scan mirrors. MATLAB was used in each step for calculation

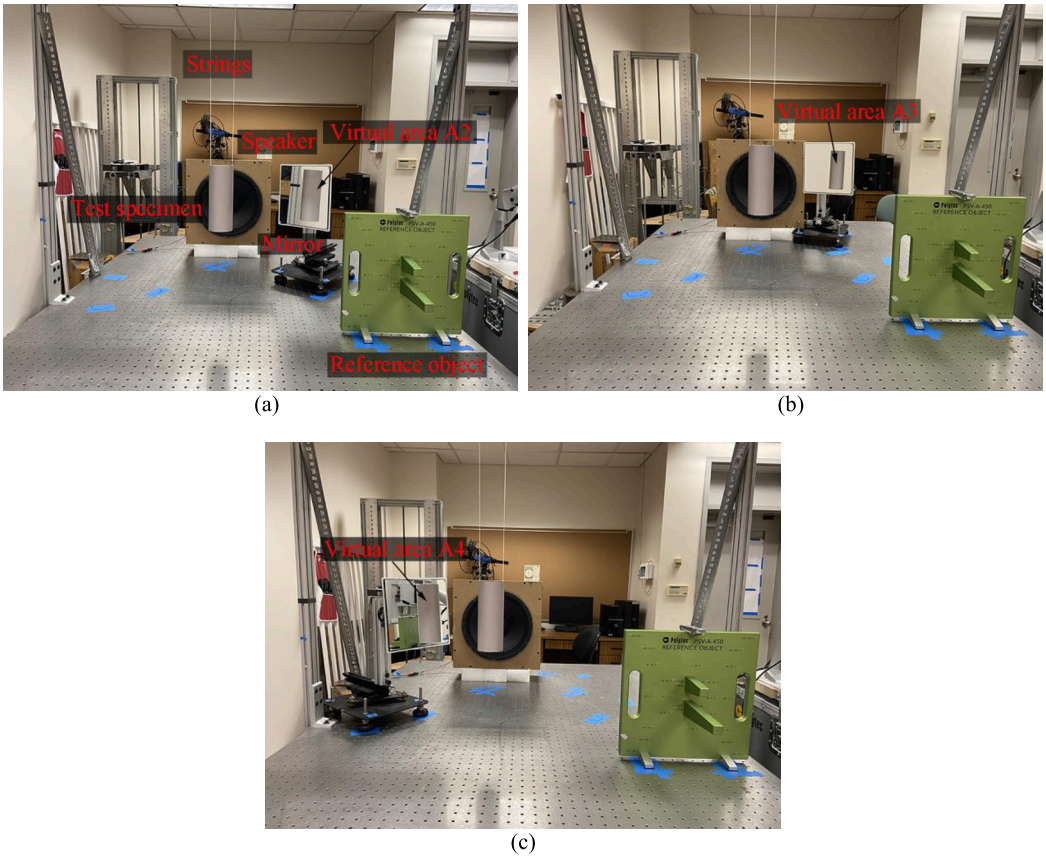

Fig. 5. Experimental setup corresponding to measurement on (a) the area A2, (b) the area A3, and (c) the area A4.

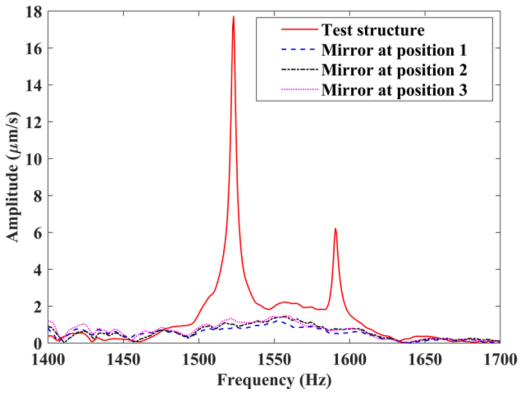

Fig. 6. Response of the test structure in the frequency domain, and those of the mirror at its three positions under periodic chirp excitation from the speaker.

and signal processing purposes. In step 1, a global MCS was defined on the reference object shown in Fig. 5, which was fixed during the experiment. Based on the global MCS, three pairs of **R** and **T** matrices for three laser heads were outputted from the system calibration to indicate their spatial relation and used to calculate the distance between each calibration point and its corresponding laser spot. A distance referred to as calibration error can be used to evaluate accuracy of the system calibration:

$$\delta^m = \|\mathbf{P}^m_{\mathrm{MCS}} - (\mathbf{T} + \mathbf{R}\mathbf{P}^m_{\mathrm{VCS}})\| \tag{7}$$

where the superscript m has the same meaning as that in Eq. (A4). Mean calibration errors from all six calibration points were 0.10 mm, 0.41 mm, and 0.10 mm for laser heads I, II, and III, respectively. Spot diameters of laser heads in this experiment were about 0.2 mm based on stand-off distances between front sides of laser heads and the reference object. One could see that mean calibration errors and laser spot diameters were of the same order.

In step 2, 3D coordinates of real areas A1-A4 of the hollow cylinder specimen and those of its virtual areas A2-A4 were captured, as shown in Fig. 8(a). Based on captured profiles of the real area A1 and virtual areas A2-A4, 3D scan trajectories can be designed in step 3 for the entire surface of the hollow cylinder specimen, as shown in Fig. 8(b). A total of four vibration acquisitions were conducted by following the order of the real area A1, the virtual area A2, the virtual area A3, and the virtual area A4. One could see from Fig. 8(b) that scan trajectories for areas A2-A4 were converted to be along the same orientation as that for the area A1, which was in the FOV of the 3D CSLDV system. Coordinates of points on scan trajectories were used to determine rotation angles of scan mirrors with Eqs. 2(a)-2(c), which were fed back to the external controller.

An index η_d based on the diameter of the measured profile of the cylinder was used to further check accuracy of profile scanning results before vibration measurement. Diameters were calculated for each plane section of the cylinder along its height. Areas A1 and A3 were used as a pair for calculation of diameters using their profile points and areas A2 and A4 were used as another pair for calculation of diameters using their profile points, as shown in Fig. 9(a), since the surface of the specimen was equally divided into four areas. The histogram of all calculated diameters was shown in Fig. 9(b). One could see that η_d lied in the range of [74.4 78.6], and its mean value and standard deviation were $\bar{\eta}_d = 75.94$ and $\widetilde{\eta}_d = 0.74$, respectively. The outer diameter of the actual specimen was 76 mm, which meant that the error between measured and actual diameters was 0.07 %. The measured geometry was highly related to the actual one and could be used in following vibration measurement. By using the diameter of the actual specimen, which is 76 mm, as a reference value, upper and lower margins of measurement errors are −2.1 % and 3.4 %, respectively. The scatter of margin values from

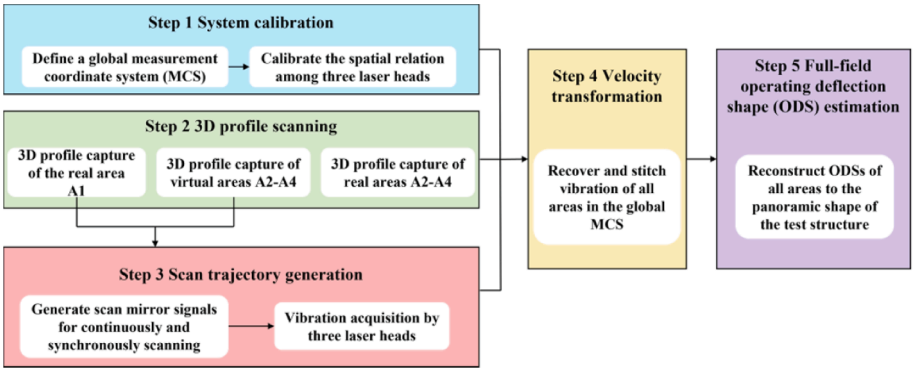

Fig. 7. Workflow of 3D CSLDV measurement of the hollow cylinder specimen using the proposed mirror-assisted testing method.

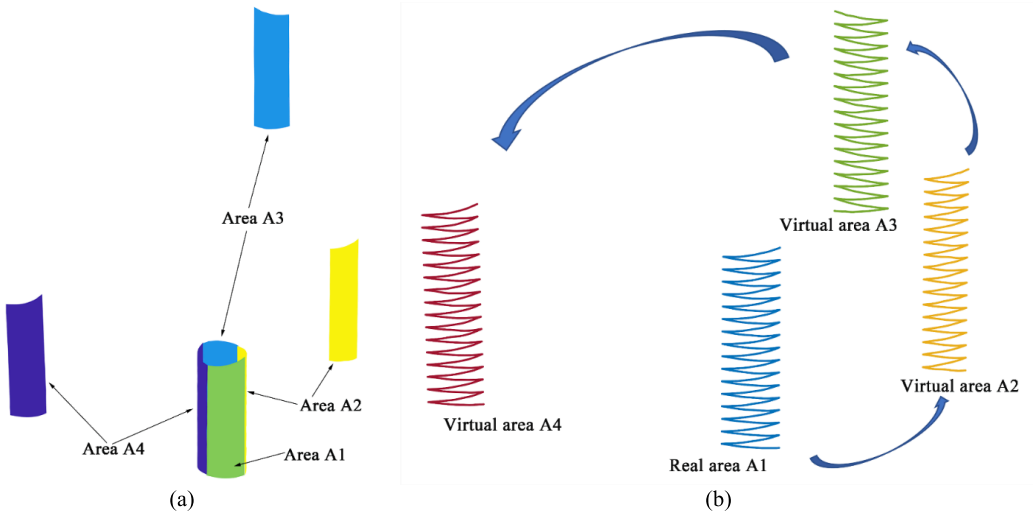

Fig. 8. (a) Profile scanning results of real areas of the hollow cylinder specimen and those of corresponding virtual areas behind the mirror, and (b) scan trajectories based on the real area A1 and virtual areas A2-A4 of the hollow cylinder specimen.

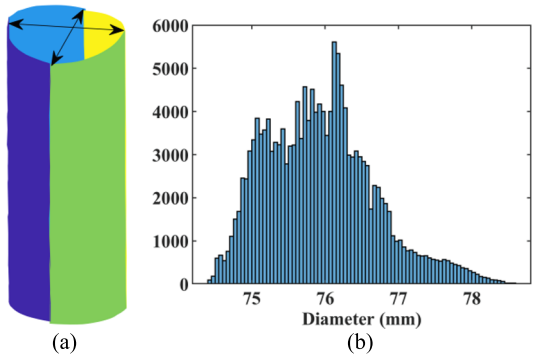

Fig. 9. (a) Schematic for calculating diameters of the measured profile of the cylinder, and (b) the histogram of calculated diameters of all plane sections of the cylinder along its height.

the reference value is due to overlaps and gaps of measurement points at boundaries between different areas.

In step 4, measured vibration of areas A2-A4 was transformed to the global MCS so that they can be stitched with that of the area A1. As proposed in Section 2.3, coordinates of three points on the mirror plane were needed for each mirror position to determine its

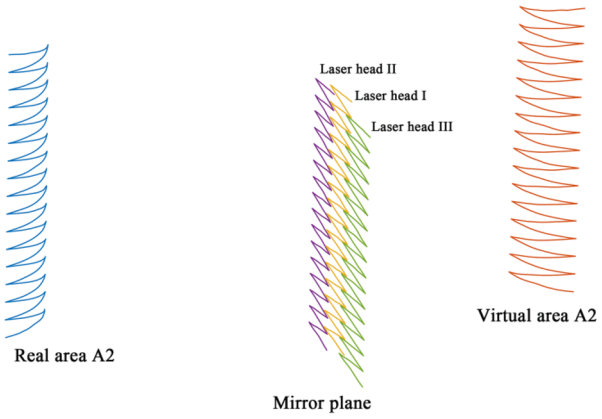

Fig. 10. Scan trajectories on real and virtual areas A2 and corresponding calculated incident scan trajectories on the mirror plane.

normal vector **n** to indicate its orientation. Three small pieces of reflective tapes were attached to three corners on the mirror so that the ranger finder and the external controller can be used to determine their coordinates by Eqs. (A1) and (A2) in the Appendix. The normal vector **n** can then be obtained by determining the cross product of two different pairs of coplanar vectors formed by three points. Obtained normal vectors were normalized to be unit vectors for indicating orientations of corresponding mirror planes. Calculated normal vectors and points on scan trajectories on virtual areas were then used to obtain coordinates of incident points on the mirror plane, as discussed in Section 2.3 and shown in Fig. 4. For instance, Fig. 10 shows scan trajectories on real and virtual areas A2, and those that contained incident points of laser beams from three laser heads on the mirror plane at its position 1. One could see that the spatial relation among three trajectories matched that of three laser heads, and scan trajectories on real and virtual areas A2 were symmetrical about the mirror plane. Virtual unit directional vectors can be obtained by using scan trajectories of incident points and the real area A2, which can then be used for transforming velocities from VCSs of three laser heads to the global MCS. As shown in Fig. 11, velocities measured by three laser heads, as shown in left three plots, were transformed to the global MCS, as shown in right three plots, for the area A2 of the hollow cylinder specimen under sinusoidal excitation with the frequency 1524 Hz. The scan frequency and sampling frequency of the measurement were 1 Hz and 10,000 Hz, respectively.

In this work, the demodulation method [2] was used to process the steady-state response of the hollow cylinder specimen from 3D CSLDV measurement under sinusoidal excitation to obtain its 3D ODSs at various excitation frequencies. The steady-state response u of the hollow cylinder specimen can be written as

$$u(\mathbf{x},t) = \Phi(\mathbf{x})\cos(\omega t - \varphi) = \Phi_{\mathrm{I}}(\mathbf{x})\cos(\omega t) + \Phi_{\mathrm{Q}}(\mathbf{x})\sin(\omega t) \tag{8}$$

where $\Phi(\mathbf{x})$ are responses at measurement points along the scan trajectory, which have two components that are the in-phase component $\Phi_{\mathrm{I}}(\mathbf{x})$ and quadrature component $\Phi_{\mathrm{Q}}(\mathbf{x})$, and φ is the phase variable. To obtain in-phase and quadrature components of $\Phi(\mathrm{x})$, multiplying $u(\mathbf{x},t)$ in Eq. (8) by $\cos(\omega t)$ and $\sin(\omega t)$ yields

$$u(\mathbf{x},t)\cos(\omega t) = 0.5\Phi_{\mathrm{I}}(\mathbf{x}) + 0.5\Phi_{\mathrm{I}}(\mathbf{x})\cos(2\omega t) + 0.5\Phi_{\mathrm{Q}}(\mathbf{x})\sin(2\omega t) \tag{9}$$

$$u(\mathbf{x},t)\sin(\omega t) = 0.5\Phi_{\mathrm{Q}}(\mathbf{x}) + 0.5\Phi_{\mathrm{I}}(\mathbf{x})\sin(2\omega t) - 0.5\Phi_{\mathrm{Q}}(\mathbf{x})\cos(2\omega t) \tag{10}$$

respectively. A low-pass filter can then be used to eliminate $\sin(2\omega t)$ and $\cos(2\omega t)$ terms in Eqs. (9) and (10), and corresponding results can be multiplied by a scale factor of two to obtain $\Phi_{\mathrm{I}}(\mathbf{x})$ and $\Phi_{\mathrm{Q}}(\mathbf{x})$, respectively. For 3D CSLDV measurement, responses $u(\mathbf{x},\mathrm{t})$ in the demodulation method can be replaced by orthogonal components of overall responses obtained from the velocity transformation to determine their ODSs. A comparison between ODSs from 3D CSLDV measurement and those from 3D SLDV measurement, which served as a quick evaluation of accuracy of the velocity transformation was conducted on the area A2. Components of 3D ODSs of the area A2 of the hollow cylinder specimen under sinusoidal excitation with the frequency 1524 Hz along x , y, and z directions of the global MCS from 3D CSLDV measurement and 3D SLDV measurement are shown in Fig. 12. One could see that results from two measurements had same levels of ratios among three components.

Components of 3D full-field ODSs of the hollow cylinder specimen under sinusoidal excitation with the frequency 1524 Hz along x , y, and z directions of the global MCS are normalized with unit maximum magnitude values and shown in Fig. 13. Based on the global MCS shown in Fig. 13, one can see that vibration of areas A1 and A3 is mainly along the z direction and vibration of areas A2 and A4 is mainly along the x direction. Vibration along the y direction that is the longitudinal direction of the hollow cylinder specimen is much smaller than that along the other two directions. Similarly, components of 3D full-field ODSs of the hollow cylinder specimen under sinusoidal excitation with the frequency 1593 Hz along x , y, and z directions of the global MCS are shown in Fig. 14. In this work, (m_1, m_2) that combines circumferential and axial modes is used to index the order of an ODS of the hollow cylinder specimen [20,23]. The former index m_1 denotes the order of its circumferential modes that equals half of the number of circumferential nodes, and the latter index m_2 denotes the order of its axial modes that equals the number of nodal circles. Magnitudes of 3D full-field ODSs of (2,0) and (2,1) modes of the hollow cylinder specimen from 3D CSLDV measurement and corresponding mode shapes from its FE model are shown in Figs. 15 and 16, respectively. Both ODSs and mode shapes are normalized by making maximum values of their overall magnitudes being unity. Modal assurance criterion (MAC) values [24] are used to indicate degrees of consistency between ODSs of the hollow cylinder specimen with free boundary conditions from the experiment and corresponding mode shapes from its FE model. In this work, MAC values for (2,0) and (2,1) ODSs and corresponding FE mode shapes are 0.99 and 0.98, respectively, which means that ODSs from the experiment and corresponding mode shapes from numerical simulation have high correlation.

4. Conclusions

This work proposes a novel mirror-assisted testing method for 3D CSLDV measurement that aims to measure 3D vibration of difficult-to-access areas of a structure without moving the 3D CSLDV system during the test, and stitch vibration of its different parts together to obtain its panoramic 3D ODSs. This work proposes a new method to design a scan trajectory for a difficult-to-access area based on coordinates of its virtual image in the mirror. Continuous and synchronous scanning of three laser spots on the difficult-to-access area can then be achieved via the method and calibration among three laser heads. This work also proposes a new method to transform vibration of the difficult-to-access area measured by three laser heads into vibration components along three orthogonal axes in a global coordinate system based on virtual positions of three laser heads. Panoramic 3D ODSs can then be achieved by stitching ODSs of different parts of the structure together since they are transformed into the same global coordinate system. The major advancement of the proposed method compared to previous studies is avoiding moving both the test structure and 3D CSLDV system,

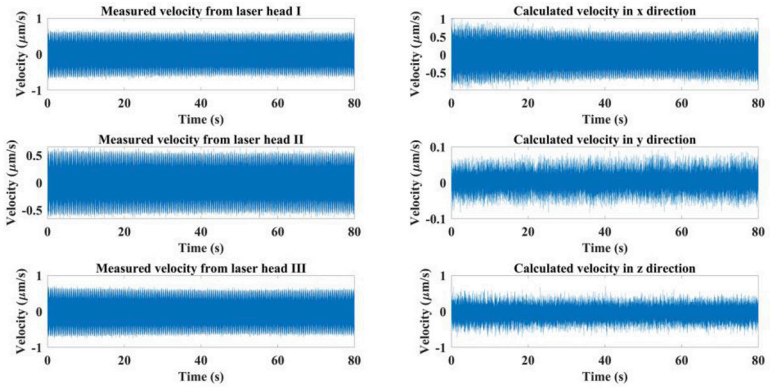

Fig. 11. Velocity transformation from three laser heads to the global MCS for the area A2 of the hollow cylinder specimen under sinusoidal excitation with the frequency 1524 Hz.

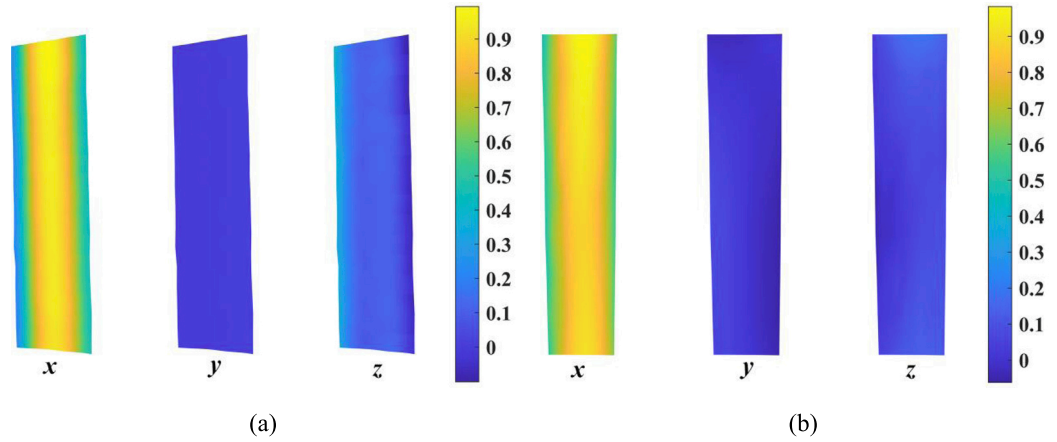

Fig. 12. Components of 3D ODSs of the area A2 of the hollow cylinder specimen under sinusoidal excitation with the frequency 1524 Hz along x ,y, and z directions of the global MCS from (a) 3D CSLDV measurement and (b) 3D SLDV measurement.

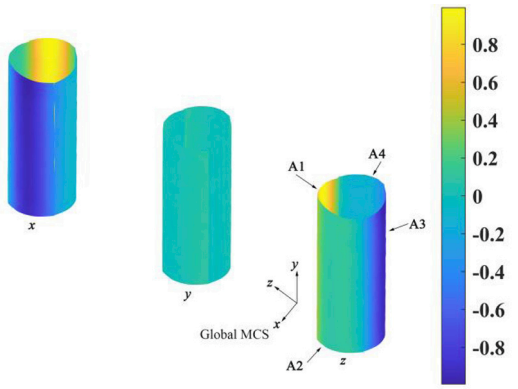

Fig. 13. Components of 3D full-field ODSs of the hollow cylinder specimen under sinusoidal excitation with the frequency 1524 Hz along x ,y, and z directions of the global MCS.

which can introduce measurement errors. Moreover, a large inner space of the test structure is not required. The proposed method can then be used in more general scenarios in practice. An experimental investigation was conducted to measure vibration of a hollow cylinder specimen with free boundaries under sinusoidal excitation and identify its panoramic 3D ODSs using the 3D CSLDV system and the proposed mirror-assisted methodology. The cylinder specimen was selected as the test structure since it represented a type of

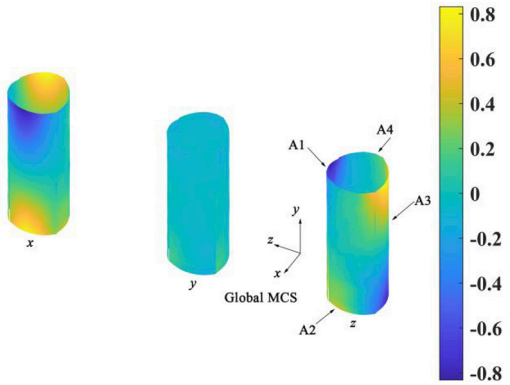

Fig. 14. Components of 3D full-field ODSs of the hollow cylinder specimen under sinusoidal excitation with the frequency 1593 Hz along x ,y, and z directions of the global MCS.

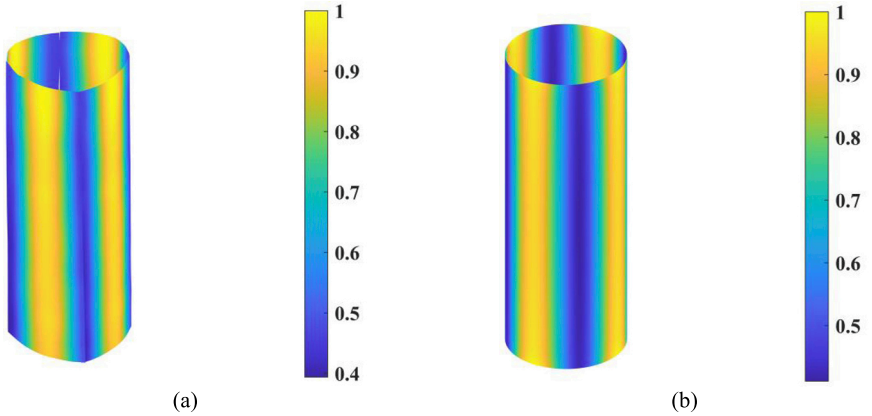

Fig. 15. (a) 3D full-field ODS of the (2,0) mode of the hollow cylinder specimen from 3D CSLDV measurement, and (b) the corresponding mode shape from its FE model.

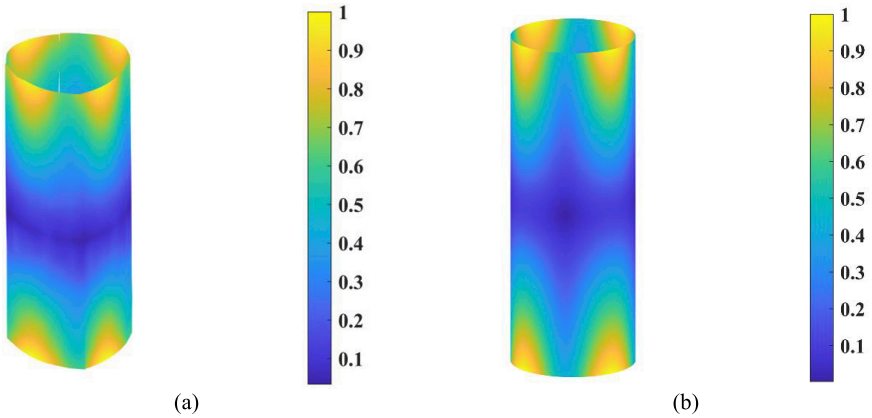

Fig. 16. (a) 3D full-field ODS of the (2,1) mode of the hollow cylinder specimen from 3D CSLDV measurement, and (b) the corresponding mode shape from its FE model.

structures whose surfaces had large curvatures and more than one difficult-to-access areas, which posed real and practical challenges for 3D CSLDV measurement. The error between measured and actual diameters of the specimen was 0.07 %, which meant that the measured geometry was highly related to the actual one and could be used in following vibration measurement. Two cases with excitation frequencies of 1524 Hz and 1593 Hz were conducted in the experiment. Results of 3D full-field ODSs of (2,0) and (2,1)

modes of the hollow cylinder specimen from the experiment have MAC values of 0.99 and 0.98 with respect to corresponding mode shapes from its FE model, which validates accuracy of the 3D CSLDV system and the proposed mirror-assisted methodology.

For most structures with complicated surfaces, the proposed method can work by dividing their surfaces into multiple areas to ensure that each area can be scanned by laser beams that are reflected by the mirror. Panoramic 3D vibration of a structure can be obtained by the vibration stitching method that is proposed and validated in this work. However, there are still problems to be resolved in the future. For example, studies on more irregular cases, such as vibration measurement of an inside surface of a structure using a mirror with an appropriate size and strategically placed orientations, are needed. In addition, for extreme cases where the mirror cannot reach some areas of the structure, the method proposed in this work can be extended by mounting the 3D CSLDV system on a multi-axis frame or a robotic arm with a precise positioning capacity, so that it can be more flexible for the 3D CSLDV system to reach more areas.

CRediT authorship contribution statement

K. Yuan: Methodology, Software, Validation, Writing – original draft. **W.D. Zhu:** Conceptualization, Funding acquisition, Methodology, Supervision, Writing – review & editing.

Declaration of competing interest

The authors declare that they have no known competing financial interests or personal relationships that could have appeared to influence the work reported in this paper.

Data availability

Data will be made available on request.

Acknowledgement

This research was supported by the National Science Foundation through Grant No. CMMI-1763024 and the Maryland Technology Development Corporation through the Maryland Innovation Initiative Grant.

Appendix

The methodology for calibrating the 3D CSLDV system, which is based on the geometrical model of the scan mirror set and a reference object Polytec PSV-A-450, is shown in Fig. A1. During the system calibration, the reference object provides a MCS that is denoted as *o-xyz*, and the scan mirror set provides a VCS that is denoted as $o'-x'y'z'$. The system calibration aims to obtain relations between coordinates of a point in the MCS $\mathbf{P}_{\mathrm{MCS}}$ and those in the VCS $\mathbf{P}_{\mathrm{VCS}}$, which can be written as

$$\mathbf{P}_{\mathrm{MCS}} = \mathbf{R}\mathbf{P}_{\mathrm{VCS}} + \mathbf{T} \tag{A1}$$

where the vector $\mathbf{T}$ with a dimension of 3×1 denotes coordinates of the VCS origin o' in the MCS, and the matrix $\mathbf{R}$ with a dimension of 3×3 is the direction cosine matrix from the MCS to the VCS.

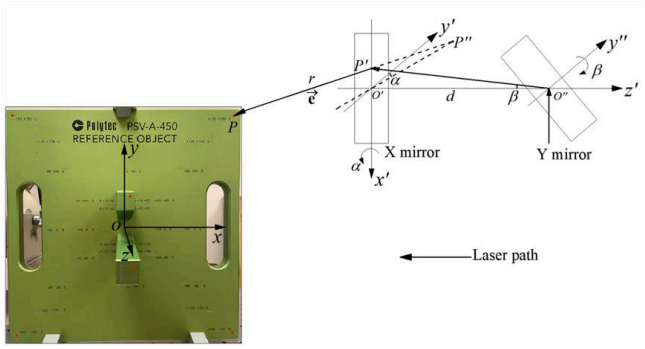

Fig. A1. System calibration based on the geometrical model of the scan mirror set and a reference object.

Six points marked in the reference object in Fig. A1 are used as calibration points in this work. Their coordinates in the MCS are $(-150, 150, 0)$, $(150, 150, 0)$, $(150, -150, 0)$, $(-150, -150, 0)$, $(-5, 25, 80)$, and $(-5, -35, 150)$. When a laser spot of a laser head is directed to one of calibration points *P* by inputting angles to scan mirrors, its coordinates in the MCS $\mathbf{P}_{\mathrm{MCS}}$ can be directly obtained from the reference object, and its coordinates in the VCS $\mathbf{P}_{\mathrm{VCS}}$ can be written as

$$\mathbf{P}_{\mathrm{VCS}} = [-d\tan\beta - r\sin\beta, -r\cos\alpha\cos\beta, -r\sin\alpha\cos\beta]^{\mathrm{T}} \tag{A2}$$

where the superscript T denotes transpose of a matrix, d is a known parameter for the laser head, α and β denote rotation angles of X and Y mirrors, respectively, and r is the measurable distance between the calibration point P and its corresponding incident point P' on the X mirror. The unit directional vector of the laser path PP' can be written as

$$\mathbf{e} = [\sin\beta, \cos\alpha\cos\beta, \sin\alpha\cos\beta]^{\mathrm{T}} \tag{A3}$$

Following steps of the system calibration include solving an over-determined nonlinear problem

$$\left|\mathbf{P}^{m}_{\mathrm{MCS}}\text{-}\mathbf{P}^{n}_{\mathrm{MCS}}\right| = \left|\mathbf{P}^{m}_{\mathrm{VCS}}\text{-}\mathbf{P}^{n}_{\mathrm{VCS}}\right| \tag{A4}$$

to obtain exact values of r for all six calibration points, where superscripts m and n are indices of calibration points, and solving an optimization problem

$$\mathrm{F}(\mathbf{T}, \mathbf{R}) = \delta = \min \sum_{m=1}^{6} \left|\mathbf{P}^{m}_{\mathrm{MCS}}\text{-}\left(\mathbf{R}\mathbf{P}^{m}_{\mathrm{VCS}}\text{-}\mathbf{T}\right)\right| \tag{A5}$$

Finally, the system calibration outputs three pairs of **T** and **R** matrices for three laser heads.

References

[1] D. Di Maio, P. Castellini, M. Martarelli, S. Rothberg, M.S. Allen, W.D. Zhu, D.J. Ewins, Continuous Scanning Laser Vibrometry: A raison d'être and applications to vibration measurements, Mech. Syst. Sig. Process. 156 (2021) 107573.
[2] A.B. Stanbridge, D.J. Ewins, Modal testing using a scanning laser Doppler vibrometer, Mech. Syst. Sig. Process. 13 (2) (1999) 255–270.
[3] M.S. Allen, M.W. Sracic, A new method for processing impact excited continuous-scan laser Doppler vibrometer measurements, Mech. Syst. Sig. Process. 24 (3) (2010) 721–735.
[4] L.F. Lyu, W.D. Zhu, Operational modal analysis of a rotating structure under ambient excitation using a tracking continuously scanning laser Doppler vibrometer system, Mech. Syst. Sig. Process. 152 (2021) 107367.
[5] L.F. Lyu, W.D. Zhu, Operational modal analysis of a rotating structure subject to random excitation using a tracking continuously scanning laser Doppler vibrometer via an improved demodulation method, J. Vib. Acoust. 144 (1) (2022) 011006.
[6] K. Yuan, W.D. Zhu, Estimation of modal parameters of a beam under random excitation using a novel 3D continuously scanning laser Doppler vibrometer system and an extended demodulation method, Mech. Syst. Sig. Process. 155 (2021) 107606.
[7] D.M. Chen, Y.F. Xu, W.D. Zhu, A comprehensive study on detection of hidden delamination damage in a composite plate using curvatures of operating deflection shapes, J. Nondestr. Eval. 38 (2019) 1–18.
[8] L.F. Lyu, K. Yuan, W.D. Zhu, A novel demodulation method with a reference signal for operational modal analysis and baseline-free damage detection of a beam under random excitation, J. Sound Vib. 571 (2024) 118068.
[9] B. Weekes, D. Ewins, Multi-frequency, 3D ODS measurement by continuous scan laser Doppler vibrometry, Mech. Syst. Sig. Process. 58 (2015) 325–339.
[10] D.M. Chen, W.D. Zhu, Investigation of three-dimensional vibration measurement by a single scanning laser Doppler vibrometer, J. Sound Vib. 387 (2017) 36–52.
[11] D.M. Chen, W.D. Zhu, Investigation of three-dimensional vibration measurement by three scanning laser Doppler vibrometers in a continuously and synchronously scanning mode, J. Sound Vib. 498 (2021) 115950.
[12] K. Yuan, W.D. Zhu, In-plane operating deflection shape measurement of an aluminum plate using a three-dimensional continuously scanning laser Doppler vibrometer system, Exp. Mech. (2022) 1–10.
[13] K. Yuan, W.D. Zhu, A novel general-purpose three-dimensional continuously scanning laser Doppler vibrometer system for full-field vibration measurement of a structure with a curved surface, J. Sound Vib. 540 (2022) 117274.
[14] K. Yuan, W.D. Zhu, Identification of modal parameters of a model turbine blade with a curved surface under random excitation with a three-dimensional continuously scanning laser Doppler vibrometer system, Measurement 214 (2023) 112759.
[15] Y. Chen, A.S. Escalera Mendoza, D.T. Griffith, Experimental dynamic characterization of both surfaces of structures using 3D scanning laser Doppler vibrometer, Exp. Tech. (2022) 1–18.
[16] B. Chen, B. Pan, Mirror-assisted panoramic-digital image correlation for full-surface 360-deg deformation measurement, Measurement 132 (2019) 350–358.
[17] B. Pan, B. Chen, A novel mirror-assisted multi-view digital image correlation for dual-surface shape and deformation measurements of sheet samples, Opt. Lasers Eng. 121 (2019) 512–520.
[18] B. Witt, D. Rohe, T. Schoenherr, Full-field strain shape estimation from 3D SLDV, in: C. Niezrecki, J. Baqersad, D. Di Maio (Eds.), Rotating Machinery, Optical Methods & Scanning LDV Methods, Volume 6, Springer, Cham, 2019.
[19] K. Yuan, W. Zhu, Modeling of welded joints in a pyramidal truss sandwich panel using beam and shell finite elements, J. Vib. Acoust. 143 (4) (2021) 041002.
[20] A.B. Stanbridge, P.R. Ind, D.J. Ewins, Measuring vibration of cylindrical surfaces using a continuous-scan LDV, in Sixth International Conference on Vibration Measurements by Laser Techniques: Advances and Applications, Volume 5503, pp. 249–259, SPIE, 2004.
[21] C.W. Schwingshackl, L. Massei, C. Zang, D.J. Ewins, A constant scanning LDV technique for cylindrical structures: Simulation and measurement, Mech. Syst. Sig. Process. 24 (2) (2010) 394–405.
[22] C. Li, Z. Zhang, Q. Yang, P. Li, Experiments on the geometrically nonlinear vibration of a thin-walled cylindrical shell with points supported boundary condition, J. Sound Vib. 473 (2020) 115226.
[23] A. Rawat, V.A. Matsagar, A.K. Nagpal, Free vibration analysis of thin circular cylindrical shell with closure using finite element method, International Journal of Steel Structures 20 (1) (2020) 175–193.
[24] D.J. Ewins, Modal testing: theory, practice and application, John Wiley & Sons, 2009.